2018

# Joganic et al 2018 AJPA Baboon heritability.pdf

James M Cheverud

Received: 15 March 2017 | Revised: 12 October 2017 | Accepted: 16 October 2017

DOI: 10.1002/ajpa.23349

RESEARCH ARTICLE

WILEY American Journal of PHYSICAL ANTHROPOLOGY

# Additive genetic variation in the craniofacial skeleton of baboons (genus *Papio*) and its relationship to body and cranial size

Jessica L. Joganic[1] | Katherine E. Willmore[2] | Joan T. Richtsmeier[3] | Kenneth M. Weiss[3] | Michael C. Mahaney[4] | Jeffrey Rogers[5] | James M. Cheverud[6]

[1]Université de Bordeaux, CNRS, MCC, De la Préhistoire à l'Actuel: Culture, Environnement et Anthropologie, (PACEA), UMR 5199, Pessac, France

[2]Department of Anatomy and Cell Biology, The University of Western Ontario, London, Ontario, Canada

[3]Department of Anthropology, Pennsylvania State University, State College, Pennsylvania

[4]South Texas Diabetes and Obesity Institute, University of Texas Rio Grande Valley School of Medicine, Brownsville, Texas

[5]Department of Molecular and Human Genetics and Human Genome Sequencing Center, Baylor College of Medicine, Houston, Texas

[6]Department of Biology, Loyola University Chicago, Illinois

**Correspondence**
Jessica L. Joganic, UMR 5199 PACEA, Université de Bordeaux, Bâtiment B8, Allée Geoffroy Saint Hilaire, CS 50023, 33615 Pessac Cedex, France.
Email: jessica.joganic@u-bordeaux.fr

**Funding information**
National Institutes of Health, Grant/Award Numbers: P01HL028972, P51RR013896, and R01RR08781; National Science Foundation, Grant/Award Numbers: BCS-0523637 and BCS-0725068

## Abstract

**Objectives:** Determining the genetic architecture of quantitative traits and genetic correlations among them is important for understanding morphological evolution patterns. We address two questions regarding papionin evolution: (1) what effect do body and cranial size, age, and sex have on phenotypic ($V_P$) and additive genetic ($V_A$) variation in baboon crania, and (2) how might additive genetic correlations between craniofacial traits and body mass affect morphological evolution?

**Materials and Methods:** We use a large captive pedigreed baboon sample to estimate quantitative genetic parameters for craniofacial dimensions (EIDs). Our models include nested combinations of the covariates listed above. We also simulate the correlated response of a given EID due to selection on body mass alone.

**Results:** Covariates account for 1.2–91% of craniofacial $V_P$. EID $V_A$ decreases across models as more covariates are included. The median genetic correlation estimate between each EID and body mass is 0.33. Analysis of the multivariate response to selection reveals that observed patterns of craniofacial variation in extant baboons cannot be attributed solely to correlated response to selection on body mass, particularly in males.

**Discussion:** Because a relatively large proportion of EID $V_A$ is shared with body mass variation, different methods of correcting for allometry by statistically controlling for size can alter residual $V_P$ patterns. This may conflate direct selection effects on craniofacial variation with those resulting from a correlated response to body mass selection. This shared genetic variation may partially explain how selection for increased body mass in two different papionin lineages produced remarkably similar craniofacial phenotypes.

**KEYWORDS**
allometry, convergent evolution, cranial evolutionary allometry, heritability, quantitative genetics

## 1 | INTRODUCTION

The fossil record for vertebrate evolution provides frequent examples of drastic changes in body size, particularly but not exclusively in island environments, where insular populations often exhibit a large increase or decrease in size relative to their mainland relatives (Foster, 1964; Lomolino, 1985; Van Valen, 1973). Many of these trends within clades have been explained by changes in diet and expansion into new niches (Gill et al., 2014; Smith et al., 2010); however, such selective pressures have also been demonstrated to directly affect craniofacial form (e.g., Burress, 2015; Cooper & Westneat, 2009; Menegaz et al., 2010). Therefore, it is often difficult to disentangle the adaptive signals

  

contained within the patterns of craniofacial and body size variation observed in extant populations to formulate valid hypotheses about the selective regimes influencing the evolution of past populations.

Genetic correlations can bias both the rate and trajectory of evolutionary responses to selection (Lande, 1979; Lande & Arnold, 1983). Depending on the magnitude of these correlations, the deviance of a population's mean phenotype from its optimal value can be substantial and result in a misinterpretation of the selective pressures that have been experienced by a population (Gould & Lewontin, 1979; Steppan, Phillips, & Houle, 2002). For example, it has been well documented that reconstructions of the phylogenetic relationships among taxa within the papionin clade differ substantially whether based on morphological or molecular data (e.g., Collard & O'Higgins, 2001; Collard & Wood, 2000; Gilbert & Rossie, 2007; Smith & von Cramon-Taubadel, 2015). This suggests that the relationship between phenotype and genotype in papionins is more complicated than initially considered.

Such cladistic incongruities are most often attributed to the confounding effects of allometry, which are acknowledged to be particularly strong in papionins (e.g., Frost, Marcus, Bookstein, Reddy, & Delson, 2003; Gilbert, 2011; Gilbert & Rossie, 2007; Leigh, 2006; Singleton, 2002). The allometry within papionins is most likely the product of sexual selection via intense male–male competition (Jolly, 1970; Leutenegger & Kelly, 1977; Lindenfors & Tullberg, 1998; Plavcan & van Schaik, 1992, 1997), although the contribution of female sexual selection cannot be dismissed and has been the subject of far fewer studies (e.g., Clutton-Brock, 2009; Rosvall, 2011). Other factors, such as diet, environment, phylogenetic inertia, and more general intrasexual interactions, have been recognized to contribute to allometric patterns in papionins as well (e.g., Clutton-Brock & Harvey, 1977; Dunbar, 1990; Lindenfors & Tullberg, 1998; Plavcan, van Schaik, & Kappeler, 1995).

Sexual dimorphism, both in body size and craniodental form, is a long-studied topic in baboons. There is evidence to support the idea that craniofacial size and shape dimorphism result from both the extension of male ontogenetic trajectories past that of females (Freedman, 1962) and the divergence of the two trajectories from each other late in adolescent development (e.g., Leigh, 2009; Leigh & Cheverud, 1991; O'Higgins & Collard, 2002). Similarly, the ontogenetic trajectories observed in the different (sub)species of baboons are parallel until later development, resulting in subtle differences that may reflect adaptations to different diets, but could be due to non-adaptive genetic drift as well (e.g., Freedman, 1963; Frost et al., 2003; Leigh, 2006). Additionally, it is evident that intergeneric differences are observable early in development in other papionin taxa. The large bodied taxa (*Papio*, *Theropithecus*, and *Mandrillus*) experience both extended ontogenetic periods and developmental trajectories that are divergent from those of the smaller bodied taxa (*Cercocebus* and *Lophocebus*; e.g., Collard & O'Higgins, 2001; Frost et al., 2003; Leigh, 2007; Singleton, 2012).

Previous work linking genotype and phenotype in the craniofacial skeleton of various primates has been conducted in humans (e.g., Carson, 2006; Martínez-Abadías et al., 2009; Sherwood et al., 2008), macaques (Cheverud, 1982; Cheverud & Buikstra, 1981a,b,1982), and callitrichids (Cheverud, 1995, 1996). Little is known, however, about the genetic underpinnings of the morphological patterns of baboon craniofacial variation. Two studies of note focus on baboons. Willmore, Roseman, Rogers, Richtsmeier, and Cheverud (2009) estimated the genetic variance underlying craniofacial phenotypic variation to be greater in male baboons, indicating they may respond more strongly to selection, even if the selection vector is the same between sexes. This is one potential explanation for the drastic sexual dimorphism observed in baboons. Furthermore, intersex genetic correlations among facial features were found to be very high ($\rho_{FM} > 0.87$), thus limiting the scope for sexual dimorphism evolution due to sexual selection. Additionally, Roseman et al. (2010) determined that estimates of genetic effects across regions of the baboon cranium are randomly distributed and, thus, any craniofacial trait is equally likely to contain phylogenetic information, although patterns of genetic covariance among traits may still bias the response to applied selection vectors.

The relationship between craniofacial and body size variation in baboons has not been systematically examined. Because the significant contribution of allometry to craniofacial variation is widely acknowledged, the allometric component of morphological variation is most often reduced in a dataset by statistical correction. The pros and cons of such practices and the resulting methodological artifacts they can produce have been widely debated (e.g., Berner, 2011; Jungers, Falsetti, & Wall 1995; Klingenberg, 2016; Richtsmeier, DeLeon, & Lele, 2002; Smith, 2005). Here, we aim to explore the biological basis for this allometric variation in baboon crania by examining the extent of the contributions of genetic correlations.

We use quantitative genetic methods to address two questions: (1) what effect do covariates, such as body and cranial size, age, and sex, have on the phenotypic and heritable (i.e., additive) genetic variation in baboon crania, and (2) how might additive genetic correlations between craniofacial traits and body size affect the evolution of the former? To our knowledge, the sample analyzed here is the largest used to date for examining the relationship between phenotypic and genetic variation in primate crania.

## 2 | MATERIALS AND METHODS

### 2.1 | Baboon sample

The sample was drawn from a colony of baboons (genus *Papio*) maintained by the Southwest National Primate Research Center (SNPRC) at the Texas Biomedical Research Institute in San Antonio, Texas. Roughly 21,000 baboons have resided at the SNPRC since the colony's establishment (MCM, pers. comm.) and of these, more than 2,400 of the animals form a single, complex pedigree for which family ancestral lines are well documented. The initial colony founders were wild-caught in southwestern Kenya, near a hybrid zone between olive (*P. hamadryas anubis*) and yellow (*P. h. cynocephalus*) baboons (Maples & McKern, 1967). The majority of current SNPRC baboons are olive baboons based on external phenotype, with some individuals displaying obvious evidence of admixture with yellow baboons (see also the discussion in Ackermann, Rogers, & Cheverud, 2006).

*Papio* taxonomy is controversial. The SNPRC follows the nomenclature suggested by Jolly (2003) in which all baboons are considered subspecies of *Papio hamadryas*. As this research uses animals from the SNPRC, that naming convention is adopted here, but we note that a growing consensus of investigators now recognize the six major baboon forms as separate species (Boissinot, Alvarez, Giraldo-Ramirez, & Tollis, 2014; Jolly, Burrell, Phillips-Conroy, Bergey, & Rogers, 2011; Zinner, Groeneveld, Keller, & Roos, 2009; Zinner, Wertheimer, Groeneveld, & Roos, 2013).

Upon death, each study monkey was necropsied by SNPRC veterinarians and its skull collected for cleaning and archiving at Washington University in St. Louis. The current collection consists of 985 skulls, of which 689 are female. All individuals were measured, but only those with both fully occluded M3's and a fused sphenoccipital synchondrosis (usually achieved by 7 years; JLJ, pers. obs.) were considered adult and included in this study. The average age of the final sample of 953 adult animals is $18.60 \pm 5.9$ years (range: 6.04–33.70 years) with females ($N = 666$) in the sample being older than males ($\bar{X}_F = 19.61 \pm 5.8$, $\bar{X}_M = 16.27 \pm 5.5$, $\bar{X}_{F-M} = 3.29$, CI = 2.5–4.0, $t = 8.24$, $p < 0.001$).

A subset of this study's sample was previously analyzed using similar methods to address a different set of research questions. Willmore et al. (2009) estimated heritability and genetic correlations between males and females using 402 of the baboons to test hypotheses about the genetic basis for cranial sexual dimorphism. However, they were unable to include calvarial traits as only data obtained from the CT scans (see below) were available. Furthermore, only 16 of the 35 traits analyzed had effective sample sizes >25 (see below) and could be included in downstream analyses. Roseman et al. (2010) estimated heritability and various measures of evolvability of 46 craniofacial traits for 410 of the baboons to determine whether any regions of the cranium are more integrated or have higher heritability estimates than others. Effective sample sizes for their genetic parameter estimations ranged from 4 to 130, with a mean of 30. Our study improves upon both of these by greatly augmenting both the census and effective sample sizes, thereby reducing the standard errors of the genetic parameter estimates and increasing power for the maximum likelihood estimation of those parameters. We were also able to include more traits in our analyses, thereby increasing the resolution in coverage of the craniofacial skeleton.

## 2.2 | Phenotyping

Because most of the calvaria were opened during necropsy, calottes were reattached with radio-translucent modeling clay. In many instances, the appearance of false start cuts on the crania permitted approximation of bone lost during necropsy, roughly 1.5 mm. A Microscribe MX (Revware Inc., Raleigh, NC) digitizer was used by JLJ to collect 3D coordinates for 28 craniometric landmarks chosen to cover the cranium completely and evenly, to be easily recognizable across the sample, and to be measured precisely on each specimen to capture craniofacial size and shape variation (Table 1; Figure 1). Twenty individuals selected at random (12 female, 8 male) were digitized twice to calculate an intraclass correlation coefficient (ICC) to assess repeatability (median ICC = 0.97).

All skulls were CT scanned at the Center for Clinical Imaging Research at Washington University School of Medicine. Endocranial volume (ECV) was estimated from the CT scans using Amira 5 (Visage Imaging, Berlin, DEU). The scans of 16 random individuals (10 female, 6 male) were segmented twice to determine ECV estimation repeatability. The average difference in repeated measures was <0.4 cubic centimeters (ICC = 0.9996).

The scans were also used to capture 21 craniometric landmarks (see Table 1 and Figure 1) using eTDIPS (see Willmore et al., 2009 for details). Seventeen of these landmarks were digitized on both dry crania and CT scans and used to assess the precision of the two methods (median ICC = 0.74). Combining both datasets results in a total of 32 unique landmarks that were assessed on each baboon cranium. Further information on landmarking can be found on the landmarks page at http://www.getahead.psu.edu.

Many of the animals lived to be very old (max age = 33.70 years), and their cranial bones remodel in response to injury, tooth loss, and age. Consequently, not all landmarks were collected for each individual and the relative location of some landmarks is affected more than others. Prosthion was most frequently absent or visibly distorted and the point was omitted from further analysis. On average, 2.6% of the remaining landmarks are missing from each individual. Euclidean inter-landmark distances (EIDs) were estimated between pairs of landmarks (Table 2) to provide measures of (1) meaningful biological units, for example, nasal length or orbital breadth; (2) traits that have been the foci of anthropological research, for example, cranial base length; or (3) dimensions for the construction of geometric objects, for example, the cranial vault versus the face. For bilateral traits and landmarks, the mean of the EIDs from each side of the cranium was used for analysis. In the case where landmarks for only one side were present, the corresponding EID for that side was substituted for the mean EID. Each EID has an average rate of missing data of 7.2% (see Table 1).

Bivariate plots for every pair of EIDs were created and examined for influential points, and any points suspected to exert undue leverage were omitted. A mean of 1.6 (median: 2, mode: 0, range: 0–5) individuals per EID were considered outlying and subsequently coded as missing data. It has been observed that animals that are hybrids between olive and yellow baboons, especially males, often demonstrate values within the tails of the population distributions, typically the right tail due to heterosis (Ackermann, Rogers, & Cheverud, 2006; Ackermann, Schroeder, Rogers, & Cheverud, 2014). Because hybrids of varying degrees are not uncommon in this sample, and because natural olive-yellow baboon hybrids have been documented in the wild (Carpentier et al., 2012), we do not treat their morphology as aberrant. Therefore, only data that were separated from the main distribution by a definitive break, as opposed to simply appearing at its tail ends, were considered outlying.

Trait distributions were non-normal (Shapiro-Wilks $W$ range: 0.88–1.00, $p < 0.001$) for all EIDs except BRPT and CNCN ($p = 0.27$ in both cases), and distributions remained non-normal for 19 of the EIDs after accounting for sex differences ($W$ range: 0.96–1.00, $p < 0.001$). In

**TABLE 1** Details of the craniometric landmarks measured on baboon crania

| Landmark | Name | Definition[a] | Locat.[b] | Reg.[c] | Miss. (%)[d] | Measur.[e] |
|---|---|---|---|---|---|---|
| Acanthion | AC | Midline of inferior margin of nasal aperture | M | F | 9.00 | JLJ, KEW |
| Anterior petrous temporal | AP | Most anterior point on inferior petrous temporal | B | B | 0.92, 0.51 | JLJ |
| Asterion | AS | Most superior point on occipitomastoid suture | B | V | 0.72, 1.74 | JLJ |
| Basion | BA | Midline on anterior margin of foramen magnum | M | B | 0.31 | JLJ, KEW |
| Bregma | BR | Intersection of sagittal and coronal sutures | M | V | 0.61 | JLJ |
| Carotid canal | CC | Most anterolateral point on inferior carotid canal foramen | B | B | 0.20, 0.31 | KEW |
| Condylion | CN | Most posteromedial point on occipital condyle | B | B | 3.07, 2.66 | JLJ, KEW |
| Crista galli anterior | CA | Most anterior point on crista galli crest posterior to orbit | M | F | 0.31 | KEW |
| Crista galli posterior | CG | Most posterior point on crista galli crest posterior to orbit | M | F | 0.41 | KEW |
| Dacryon | DA | Most superior point on lacrimomaxillary suture | B | F | 0.41, 0.31 | JLJ |
| Frontomalare orbitale | FM | Intersection of frontozygomatic suture and lateral orbital rim | B | F | 0.31, 0.51 | JLJ, KEW |
| Jugale | JP | Most anterior point on occipital jugular notch | B | B | 0.51, 0.51 | JLJ |
| Lambda | LD | Intersection of sagittal and lambdoid sutures | M | V | 0.82 | JLJ |
| Maxillary tuberosity | MX | Point where inferior palatomaxillary suture crosses M3 midline | B | F | 0.72, 0.82 | JLJ, KEW |
| Nasale | NL | Most inferior point on inter-nasal suture | M | F | 2.66 | JLJ, KEW |
| Nasion | NA | Intersection of inter-nasal and frontal sutures | M | F | 0.41 | JLJ, KEW |
| Opisthion | OP | Midline on posterior margin of foramen magnum | M | B | 7.06 | JLJ, KEW |
| Orbital septum | OB | Intersection of orbital septum and medial orbital wall | B | F | 0.72, 0.72 | JLJ |
| Palatale | PL | Most posterior point on palatal surface of inter-maxillary suture | M | F | 0.20 | JLJ |
| Porion | PO | Intersection of ectotympanic and tympanic petrous | B | V | 11.15, 3.99 | JLJ, KEW |
| Premaxilla/maxilla junc. | PM | Most anterior point on inferior premaxilla-maxillary suture | B | F | 12.68, 14.52 | JLJ, KEW |
| Premolar/molar junc. | 41 | Most inferior point on alveolus between P4 and M1 | B | F | 4.40, 4.91 | JLJ, KEW |
| Prosthion | PR | Most anterior point on lingual surface of maxillary I1 septum | M | F | 14.21 | JLJ, KEW |
| Pterion | PT | Most inferior point on coronal suture | B | V | 3.07, 1.64 | JLJ |
| Sella turcica | SL | Center of sella turcica | M | F | 0.20 | KEW |
| Staphylion | SY | Most posterior point on vomeropalatal suture | M | F | 1.43 | JLJ, KEW |
| Stephanion | ST | Intersection of superior temporal line and coronal suture | B | V | 0.61, 0.61 | JLJ |
| Temporosphenoid junc. | TS | Most superior point on temporosphenoid suture | B | V | 0.20, 0.41 | JLJ |
| Vomerosphenoid junc. | VS | Most posterior point on vomeral alae intersection | M | B | 0.31 | JLJ, KEW |
| Zygomaxillare inferior | ZI | Most inferior point on zygomaxillary suture | B | F | 0.20, 0.82 | JLJ, KEW |
| Zygomaxillare superior | ZS | Intersection of zygomaxillary suture and inferior orbital rim | B | F | 0.20, 0.31 | JLJ, KEW |
| Zygotemporal junc. | ZT | Intersection of zygotemporal suture and superior zygomatic arch | B | F | 1.02, 1.74 | JLJ, KEW |

[a]Adapted from "*A laboratory manual of anthropometry*," by Wilder, 1920, Philadelphia, PA: P. Blakiston's Son & Company.
[b]Whether the landmark is bilateral (B) or in the midline (M).
[c]Region of the skull in which the landmark is located: base (B), face (F), and vault (V).
[d]Percent missing data. Bilateral landmarks have a number each for the right and left sides.
[e]Coauthor who measured the landmark on either dry crania (JLJ) or CT scans (KEW). Placement of these landmarks can be visualized in Figure 1 and at http://getahead.psu.edu/viewer.html?id = Baboon_Skull.

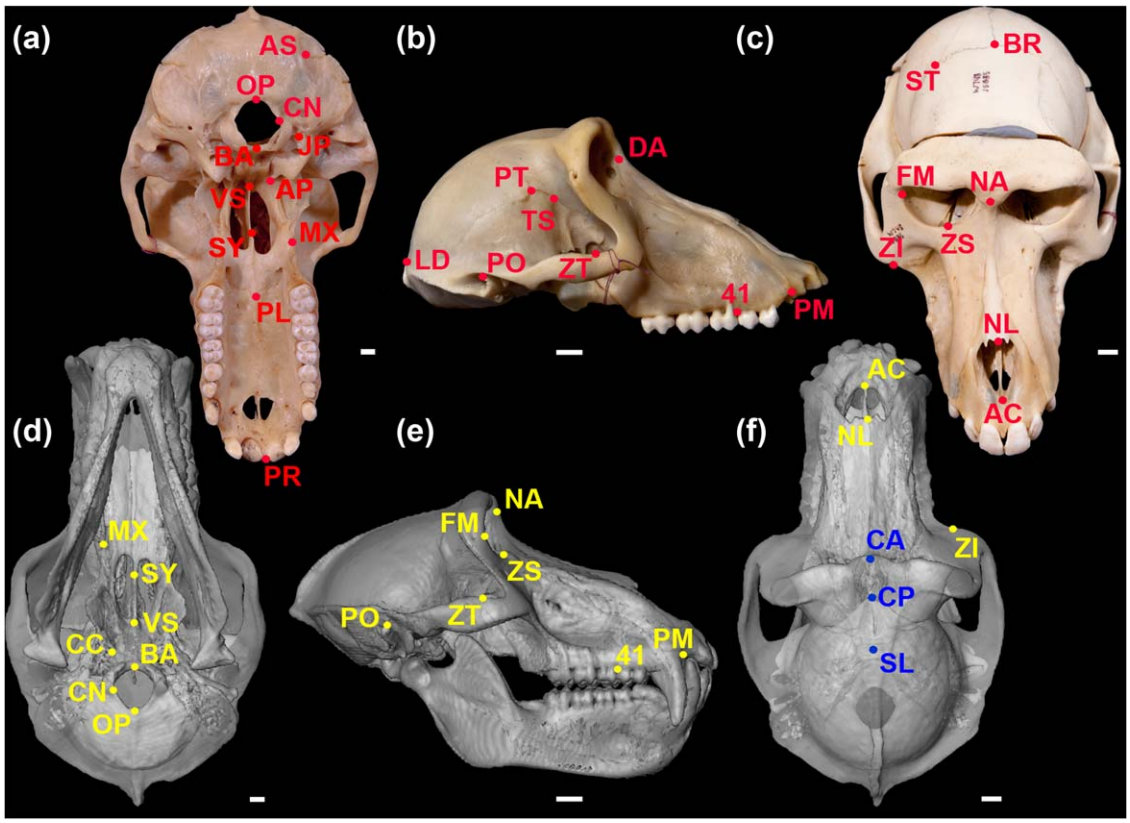


**FIGURE 1** Craniometric landmarks collected. Panels: (a–c) Landmarks (red dots and letters) collected with a microscribe by JLJ from the dry crania, inferior view (a), right lateral view (b), and oblique superior view (c). (d–f) Landmarks (yellow and blue dots and letters) collected digitally by KEW from the CT scans, inferior view (d), right lateral view (e), superior view (f). Abbreviations correspond to those provided in Table 1. Blue landmarks are endocranial while red and yellow landmarks are ectocranial. Only the right side of bilateral landmarks is identified in each of the images. Orbital septum (OB) is not shown. White scale bars are 1 cm. Photographs by Aaron Bunse and transparent virtual skulls reconstructed from CT scans by KEW

many cases, trait distributions were heavily leptokurtic, most often demonstrating a positive skew. This is an issue for maximum likelihood estimation of the quantitative genetic parameters, as analyzed traits are assumed to be multivariate normal. Therefore, the residuals obtained after controlling for body mass and other covariates that significantly structure each EID, such as sex and age, were transformed to fit an inverse Gaussian distribution, which is suitable for modeling in instances where large trait values are more probable than is the case for a typical Gaussian distribution. This process of inverse normalization produces phenotypes (iEIDs) that are comparable across both individuals and traits by directly normalizing residuals to obtain standard normal quantile values.

## 2.3 | Body and cranial size

Scaling relationships between craniofacial measurements and body size are important to consider in morphological research, particularly for *Papio*, as body size sexual dimorphism is extreme (e.g., Leigh, 2009; Willmore et al., 2009) and contributes significantly to phenotypic correlation structure in the baboon cranium (Porto, de Oliveira, Shirai, De Conto, & Marroig, 2009). It is possible to identify the genetic architecture of phenotypic variation in the baboon cranium that is attributable to genetic variants affecting craniofacial variation alone by controlling for body size while estimating quantitative genetic parameters. To do so, a proxy measurement for the body size of each individual in the sample must be estimated (e.g., body mass, crown-rump length, femoral head diameter).

Individual body mass measurements were obtained for each baboon. Iterative piecewise regression (IPR) was used to first estimate the sample-wide age of growth cessation from longitudinal body mass data provided by the SNPRC ($N = 42{,}838$ records). IPR models a quadratic growth curve for the growth portion of the data, an asymptotic adult size, and an inflection point between the two, which represents the age at growth cessation (O'Mara, Gordon, Catlett, Terranova, & Schwartz, 2012). Once the sex-specific inflection points were identified (F: 10.67 years, M: 7.68 years; Joganic, 2016; Leigh, 2009), the body mass recorded closest to the appropriate inflection point ± 2 years was used as an individual's adult body mass. In instances where two records were equally close to the growth-cessation estimate, a mean body mass was calculated.

A variety of methods have been employed for estimating overall cranial size: for example, centroid size of landmark coordinate data, geometric mean of cranial size dimensions, ECV or brain size, cranial base length, and the first principal component (PC) from a PC analysis (PCA)

**TABLE 2** EIDs calculated between craniometric landmarks and their repeatability estimates

| EID[a] | Repeat[b] | EID | Repeat | EID | Repeat |
|---|---|---|---|---|---|
| BRNA* | 0.978 | SYBA | 0.995 | ACSY | 0.996 |
| BRPT* | 0.546 | VSBA* | 0.989 | FMPM | 0.992 |
| PTPT* | 0.858 | ASJP* | 0.859 | NA41 | 0.995 |
| STST | – | BACC | – | NAAC | 0.996 |
| BRBA | 0.967 | BAOP | 0.925 | NANL* | 0.996 |
| NALD | 0.842 | CNCN | 0.958 | NAZI | 0.974 |
| PTAS* | 0.857 | JPJP* | 0.963 | NLAC | 0.990 |
| PTLD* | 0.769 | LDBA* | 0.989 | NLVS | 0.998 |
| ASAS* | 0.802 | POBA | 0.990 | ZSNL | 0.998 |
| BRAS* | 0.910 | POPO* | 0.991 | CPZS | – |
| BRLD* | 0.814 | 4141 | 0.981 | DAFM | 0.968 |
| LDAS* | 0.914 | 41MX | 0.976 | FMCP | – |
| CACP | – | 41ZI | 0.977 | FMPT* | 0.769 |
| CPSL | – | ACPM | 0.837 | NAFM | 0.995 |
| NABA | 0.986 | PLSY | 0.960 | NAZS | 0.948 |
| NACA | – | PM41 | 0.860 | FMZT* | 0.988 |
| NACP | – | PMPM | 0.996 | ZTPO | 0.946 |
| NAVS | 0.954 | SYMX | 0.971 | ZTVS | 0.997 |
| SLBA | – | VSSY | 0.972 | ZTZI* | 0.841 |
| SLCC | – | ZIMX | 0.876 | ZTZT | 0.998 |

[a]EIDs indicated with an asterisk were also present in the Cayo Santiago macaque dataset and used in analyses addressing research question 2.
[b]ICCs calculated from a subset of EIDs that were measured twice by JLJ to assess repeatability. EIDs indicated with a dash were measured exclusively by KEW and duplicate trials were not conducted.

of cranial size dimensions. However, the use of linear distances, rather than 3D coordinate data, precludes the estimation of a centroid size and the presence of negative values in the inverse-normalized EIDs prevents calculation of the geometric mean. Additionally, both ECV and cranial base length (NABA; see Table 2) are variables of interest, so they cannot be treated as control variables. Given these limitations, PCA was used to extract the first PC, generally considered to contain primarily size-related variation, for use as a surrogate of cranial size.

PCA was performed on the 60x60 pairwise-complete correlation matrix of iEIDs ($M_P$) in RStudio v 1.0.136 (RStudio Team, 2016). The PC1 eigenvalue is 10.01 and accounts for 17% of the variation in $M_P$. Its loadings were examined to determine which cranial dimensions best quantify size variation in the baboon cranium (Supporting Information Table S1; Figure 2). iEIDs scoring highest on PC1 capture variation in snout length (ACSY, FMPM, NA41, NAAC, NLVS, and ZSNL), cranial base length (NABA and NAVS), facial breadth (NAZI, ZTVS, and ZTZT), and facial hafting, or the angle at which the face attaches to the neurocranium (FMCP and NACP). This result suggests that facial variation dominates baboon craniofacial variation beyond that attributed to the marked facial size sexual dimorphism that characterizes *Papio*, which was accounted for by controlling for sex differences when calculating iEIDs.

Because only 360 individuals have values for all 60 iEIDs, component scores could not be calculated for every cranium from the PCA of $M_P$. Instead, multiple imputation was used to fill holes in the dataset by creating a predictive model that included all the information available in the observed data and any *a priori* knowledge about data structure. Expectation-Maximization with Bootstrapping was used to impute missing data in the R package Amelia II (Honaker, King, & Blackwell, 2011), producing a final dataset ($N = 880$) with no missing data (Supporting Information Materials S1). From this final imputed dataset, $M_P$ PC1 scores were calculated to be used as a proxy for cranial size.

## 2.4 | Heritability

Heritability estimates were obtained by maximum likelihood variance decomposition (MLVD) using the program Sequential Oligogenic Linkage Analysis Routines (SOLAR v 8.8.1; Almasy & Blangero, 1998). Using the genetic information contained in the baboon pedigree and the phenotypic variance ($V_P$) reflected in the craniofacial measurements, SOLAR estimates genetic variance ($\sigma_g^2$) for each trait by maximizing the likelihood of the model:

$$\Omega = 2\Phi\sigma_g^2 + I\sigma_e^2 \quad (1)$$

where $\Omega$ is the pedigree covariance matrix providing the expected phenotypic covariance between pairs of individuals, $\Phi$ is the kinship matrix derived from the pedigree and composed of Cotterman's (1940) pairwise kinship coefficients ($k$), $I$ is an identity matrix, and $\sigma_e^2$ is the variance in random environmental effects. This variance is assumed to be uncorrelated among individuals because all pedigreed baboons are housed in the same environment at the SNPRC. The resulting parameter of interest is the estimate of residual heritability ($h_r^2$), or the proportion of $V_P$ accounted for by $\sigma_g^2$ after removing any variation attributable to covariates, such as sex and age.

Because the individuals in this sample are related, the estimated trait values are not independent of each other. As a result, the effective sample size ($N_e$) is the only truly important number for determining the efficiency of quantitative genetic parameter estimates. It measures the effective number of individual breeding values used in the analysis (i.e., the amount of genetically independent information contained in the data). Estimates of $N_e$ were made using the methodology of Cheverud (1995):

$$N_e = \frac{2h^4}{V(h^2)} + 1 \quad (2)$$

where $h^4$ is the square of heritability and $V(h^2)$ is its variance (i.e., square of the standard error).

## 2.5 | Research question 1: The effect of allometric variation

Three nested models were used to determine the effect of different covariates on the distribution patterns of phenotypic and genetic

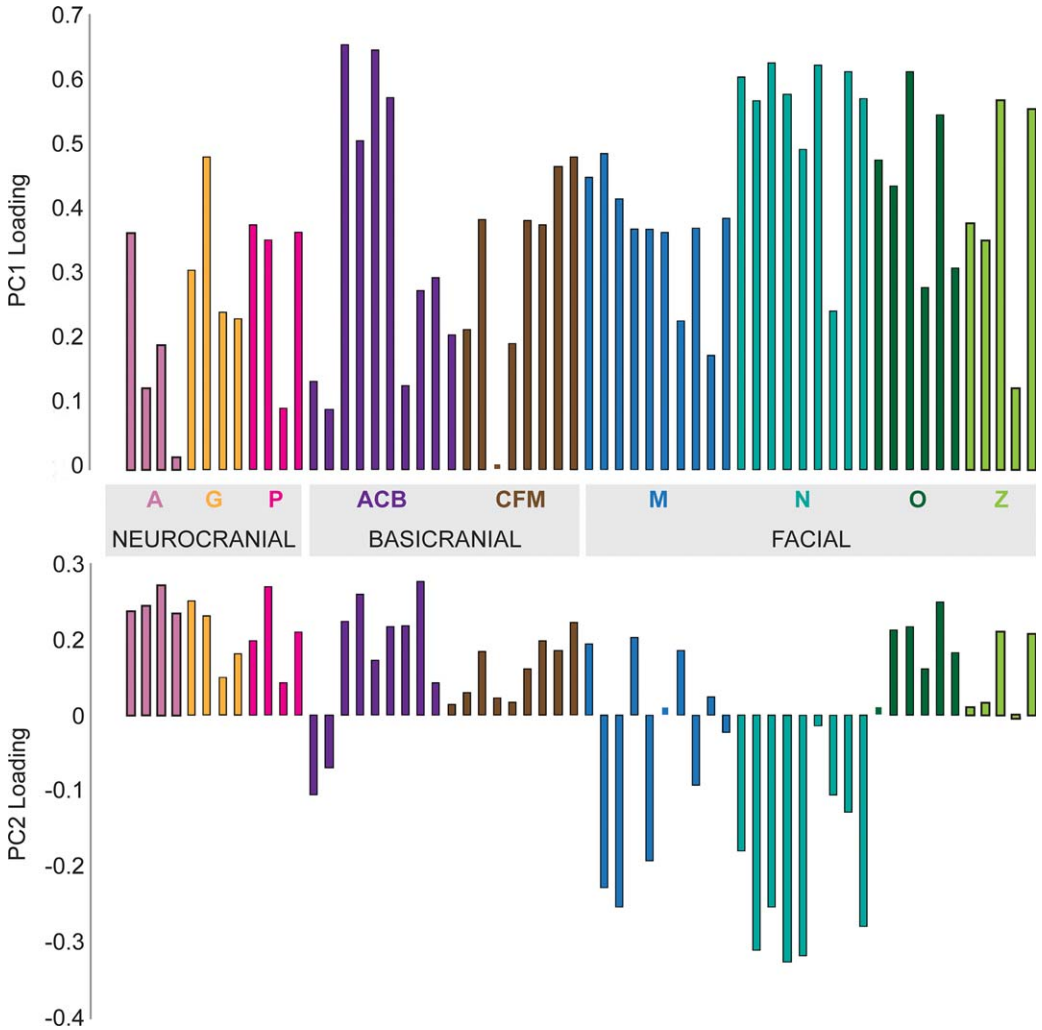


**FIGURE 2** Standardized loadings for each of the 60 iEIDs on the first two eigenvectors of a PCA performed on the pairwise-complete correlation matrix ($M_P$). The iEIDs are grouped and colored by cranial region: anterior neurocranium (A), global neurocranium (G), and posterior neurocranium (P); anterior cranial base (ACB) and circum-foramen magnum (CFM); oral (M), nasal (N), orbital (O), and malar (Z)

craniofacial variation. Model 1 examines craniofacial variation as it relates to variation in the entire body due to systemic effects (e.g., sex hormones and ontogenetic changes). Five basic variables were included as potential covariates: sex, age, the interaction between sex and age, the square of age to account for nonlinearity (age$^2$), and the interaction between sex and age$^2$. The effects measured here include local regional cranial effects, overall cranial size effects, and overall body size effects.

Model 2 eliminates any whole-body effects operating on the cranium by including adult body mass in addition to the five aforementioned covariates in the model. Remaining variation would then include the effects of factors contributing to overall cranial size in a manner that is independent of allometric scaling within the cranium related to overall body size. For example, the systemic effects of circulating hormones on the overall size of an individual would be accounted for in Model 2. Any additional size and shape variation of specific craniofacial regions, such as variation of the zygomatic arches and neurocranial vault resulting from osteoblastic activity in response to differential muscle forces caused by the anabolic influences of such hormones, would remain.

Model 3 eliminates whole cranium allometric effects, which are particularly strong in baboons (e.g., Frost, Marcus, Bookstein, Reddy, & Delson, 2003; Leigh, 2006; Leigh & Cheverud, 1991; O'Higgins & Collard, 2002; Singleton, 2002). The effects of cranial size and size-related shape variation are removed by including cranial size (i.e., the PC1 scores) as a covariate in addition to the six that were included previously in Model 2. This focuses the model on variation in smaller regions of the baboon cranium (e.g., orbit; anterior cranial base, ACB), which likely correspond to functional, developmental, and/or genetic/evolutionary modules.

For each trait, the proportion of phenotypic variation attributable to covariates ($V_{cov}$) was estimated and removed ($V_P - V_{cov}$) to produce the residual phenotypic variance ($V_{Pr}$). Therefore, heritability in this case is defined as the proportion of $V_{Pr}$ due to additive genetic variance ($V_A$). However, because $h_r^2$ is a ratio, increases in its magnitude from one model to the next or among traits can be the result of larger $V_A$, smaller environmental variance ($V_{Pr} - V_A$), or a combination of the two (Houle, 1992). For this reason, $V_A$ was estimated as the product of $h_r^2$ and $V_{Pr}$ to create a metric for comparing relative amounts of genetic

variation alone. For traits in Model 1 that do not have any significant covariates, $V_P$ was used instead of $V_{Pr}$.

Finally, additive genetic correlations ($\rho_G$) between each iEID and adult body mass (kg) were estimated to determine the amount of shared genetic variation. Correlation estimates were obtained in SOLAR by fitting a bivariate model to each of the 60 iEIDs paired in turn with body mass and including age, sex, and their interaction terms (see the description of Model 1 above) as covariates. In other words, 60 estimates of $\rho_G$(iEID, kg) were obtained.

To identify any regional patterns in the distribution of covariate effects, we performed a joint hierarchical cluster analysis for mixed categorical and continuous data (Gower, 1971). For every pair of traits *i* and *j*, a similarity coefficient ($S_{ij}$) was estimated (Supporting Information Materials 2). The Unweighted Pair-Group Method with Arithmetic Means (UPGMA) was used to cluster the matrix of $S_{ij}$ coefficients and a cophenetic correlation coefficient was estimated to determine how faithfully the clustering algorithm captured the variation in the original data. Dendrograms were created from the cophenetic distances produced by the UPGMA algorithm and examined to discern any trends in trait similarity across the cranium. Data visualization and all analyses were conducted using custom Python scripts (Supporting Information Materials 3).

### 2.6 | Research question 2: Correlated response to selection on body mass

We investigated the potential for selection on body mass to produce a correlated response in craniofacial shape because of shared genetic variation using Falconer and MacKay's (1996) equation for $CR_y$:

$$CR_y = ih_x\rho_G\sigma_{Ay} \quad (3)$$

where body mass in kg is variable *x*, the relevant iEID is variable *y*, *i* is the selection intensity, $h_x$ is the square root of the heritability of body mass, $\rho_G$ is the additive genetic correlation between the two traits, and $\sigma_{Ay}$ is the square root of the additive genetic variance of the iEID in question. The heritability of body mass was estimated by MLVD in SOLAR using the same methodology as for the iEIDs (body mass $h^2_r = 0.433$). The magnitude of *i* is arbitrary and we used two different values. First, because a low amount of selection will produce next generation means that do not differ appreciably from the average rhesus macaque values, we set $i = 100$. *Macaca* was selected because it is typically considered to retain the most ancestral morphology of the papionin clade (Disotell, 1992; Harris, 2000; Tosi, Disotell, Morales, & Melnick, 2001; although see Singleton, 2002). Then, to create a more realistic scenario, we set $i = 5.28$, the number of within-species standard deviations in body mass separating macaques ($\bar{X}_F = 5.4$ kg, $\bar{X}_M = 7.7$ kg; MacDonald, 2001) from the SNPRC baboons ($\bar{X}_F = 18.75$ kg $\pm$ 3.5, $\bar{X}_M = 29.08$ kg $\pm$ 4.1; this study). This ensures that selection is strong enough to account for overall difference in body mass between the species.

Next, the mean shapes of both a male and female rhesus macaque were calculated from data collected using sliding calipers by JMC from the free-ranging colony on Cayo Santiago. Only a subset of 18 EIDs were common to both the macaque and baboon datasets (see Table 2) and, thus, were used in this analysis.

Each sex-specific mean EID was modified by the corresponding $CR_y$ to simulate a single round of direct selection on body mass in the parental population possessing the ancestral morphotype (i.e., macaques) to produce a next generation craniofacial morphology modified via indirect response to selection on body mass alone. Pearson correlation coefficients were calculated between the vectors of "offspring" generation values and those of the sex-specific mean baboon EIDs. If size selection was the only cause of evolutionary change, the sum of the vector of $CR_y$ coefficients and the macaque vector should equal the baboon vector. Therefore, a high correlation between the next generation and the baboon vectors indicates that the pattern of craniofacial variation observed in our baboon sample can be explained adequately by a simple model of correlated response to indirect selection on body mass in ancestral papionin populations. Lower correlation coefficients suggest that selection on size alone will not move a population from the morphospace region inhabited by macaques to that inhabited by baboons. Therefore, additional selection scenarios involving direct selection on individual craniofacial traits or selection on other, unspecified traits correlated with the craniofacial traits must be invoked as well.

## 3 | RESULTS

Quantitative genetic parameters were estimated for ECV and 60 traits quantifying size and shape variation in baboon crania (Table 3) using MLVD. The $h^2_r$ estimates (Supporting Information Table S2) for the baboon craniofacial traits are consistent with expectations based on the typical heritability of most morphological traits in vertebrates. This is estimated to be ~0.40 (e.g., Berry et al., 2003; Cheverud, 1996; Cheverud et al., 1990; Kruuk et al., 2002; Mousseau & Roff, 1987; Safari, Fogarty, & Gilmour, 2005; Visscher, Thompson, & Hill, 1991). The mean $h^2_r$ estimates across traits for each model are $\bar{h}^2_{r1} = 0.48 \pm 0.2$, $\bar{h}^2_{r2} = 0.45 \pm 0.2$, $\bar{h}^2_{r3} = 0.42 \pm 0.1$. Heritability estimates in all three models are statistically significant meaning additive genetic variation ($V_A$) contributes to $V_{Pr}$ for all baboon craniofacial traits.

### 3.1 | Effective sample size

Effective sample sizes range from 8.9 to 301.3, depending on the trait and the level of analysis (see Supporting Information Table S2). The geometric mean $N_e$ in each model is: $\bar{X}_{G1} = 75.9 \pm 59$, $\bar{X}_{G2} = 60.1 \pm 50$, and $\bar{X}_{G3} = 56.4 \pm 39$. The decrease in $N_e$ between Models 1 and 2 is marginally significant ($t = 1.92$, $p = 0.057$) but that between Models 2 and 3 is not ($t = 0.98$, $p = 0.33$). As effective sample size is an estimate of the amount of genetic information available for each character, this slight reduction in $N_e$ resulting from including body mass as a covariate in Model 2 suggests that at least a portion of the underlying genetic variance affects both body mass and craniofacial variation.

**TABLE 3** Descriptive statistics for baboon craniofacial traits

| Trait | BRNA | BRPT | PTPT | STST | BRBA | NALD | PTAS | PTLD | ASAS | BRAS | BRLD | LDAS | CACP | CPSL | NABA |
|---|---|---|---|---|---|---|---|---|---|---|---|---|---|---|---|
| Mean[a] | 62.51 | 44.46 | 58.44 | 30.44 | 67.86 | 101.77 | 55.39 | 69.93 | 60.09 | 60.47 | 47.08 | 38.77 | 16.77 | 17.52 | 80.66 |
| SD | 4.1 | 3.5 | 3.0 | 9.3 | 3.8 | 6.6 | 3.9 | 5.0 | 5.9 | 4.1 | 5.3 | 5.1 | 1.9 | 1.9 | 6.0 |
| Min | 50.33 | 32.55 | 49.4 | 2.6 | 58.95 | 88.74 | 46.46 | 58.44 | 44.38 | 50.74 | 34.71 | 28.2 | 11.39 | 13.28 | 68.09 |
| Max | 75.5 | 54.28 | 67.69 | 54.48 | 79.75 | 127.59 | 68.58 | 89.66 | 82.9 | 74.73 | 68.34 | 56.86 | 21.66 | 23.74 | 99.43 |
| N | 935 | 934 | 904 | 943 | 937 | 933 | 940 | 939 | 927 | 936 | 931 | 936 | 941 | 941 | 942 |
| **Trait** | **NACA** | **NACP** | **NAVS** | **SLBA** | **SLCC** | **SYBA** | **VSBA** | **ASJP** | **BACC** | **BAOP** | **CNCN** | **JPJP** | **LDBA** | **POBA** | **POPO** |
| Mean | 25.37 | 42.08 | 52.2 | 25.47 | 27.33 | 40.2 | 30.29 | 39.22 | 19.76 | 19.54 | 18.01 | 20.89 | 60.83 | 46.7 | 77.27 |
| SD | 2.8 | 3.0 | 4.1 | 3.6 | 2.9 | 4.2 | 3.2 | 3.6 | 1.6 | 2.1 | 1.4 | 1.9 | 5.8 | 4.6 | 8.1 |
| Min | 18.41 | 35.51 | 43.35 | 16.7 | 21.14 | 29.51 | 22.75 | 28.39 | 16.29 | 14.29 | 14.51 | 16.48 | 50.54 | 38.09 | 64.44 |
| Max | 33.35 | 52.21 | 66.34 | 35.4 | 35.49 | 52.97 | 40.77 | 49.96 | 25.08 | 26.24 | 22.43 | 26.59 | 78.48 | 58.62 | 102.39 |
| N | 938 | 932 | 938 | 944 | 943 | 932 | 935 | 937 | 947 | 876 | 938 | 934 | 932 | 944 | 821 |
| **Trait** | **4141** | **41MX** | **41ZI** | **ACPM** | **PLSY** | **PM41** | **PMPM** | **SYMX** | **VSSY** | **ZIMX** | **ACSY** | **FMPM** | **NA41** | **NAAC** | **NANL** |
| Mean | 48.46 | 45.1 | 43.25 | 21.16 | 30.28 | 26.96 | 32.63 | 21.72 | 14.45 | 31.02 | 81.08 | 91.45 | 85.26 | 89.56 | 59.01 |
| SD | 4.1 | 4.0 | 5.8 | 2.6 | 5.4 | 4.4 | 3.7 | 2.5 | 2.6 | 4.7 | 10.2 | 11.1 | 9.9 | 12.0 | 9.7 |
| Min | 40.65 | 33.54 | 31.24 | 16.25 | 19.39 | 20.34 | 22.78 | 16.82 | 8.16 | 21.92 | 61.56 | 70.34 | 65.14 | 66.24 | 40.02 |
| Max | 59.93 | 57.76 | 62.25 | 29.63 | 46.93 | 41.31 | 46.08 | 29.48 | 23.46 | 46.58 | 106.64 | 126.41 | 114.4 | 124.49 | 85.03 |
| N | 937 | 915 | 930 | 918 | 931 | 931 | 799 | 928 | 933 | 940 | 847 | 933 | 916 | 858 | 938 |
| **Trait** | **NAZI** | **NLAC** | **NLVS** | **ZSNL** | **CPZS** | **DAFM** | **FMCP** | **FMPT** | **NAFM** | **NAZS** | **FMZT** | **ZTPO** | **ZTVS** | **ZTZI** | **ZTZT** |
| Mean | 62.4 | 33.31 | 72.86 | 49.27 | 41.28 | 33.54 | 46.22 | 28.93 | 37.47 | 29.84 | 35.38 | 47.17 | 50.5 | 21.18 | 96.39 |
| SD | 5.1 | 4.0 | 9.4 | 8.8 | 3.0 | 2.2 | 3.7 | 3.9 | 2.7 | 2.4 | 3.4 | 5.2 | 5.2 | 4.4 | 9.9 |
| Min | 52.88 | 23.84 | 57.43 | 31.07 | 34.75 | 29.4 | 39.69 | 19.35 | 31.36 | 23.21 | 28.44 | 36.97 | 41.71 | 12.32 | 79.46 |
| Max | 78.69 | 45.88 | 99.59 | 72.37 | 50.07 | 39.72 | 57.18 | 42.17 | 45.68 | 37.5 | 46.38 | 64.01 | 65.47 | 35.36 | 122.9 |
| N | 936 | 915 | 915 | 938 | 940 | 936 | 937 | 938 | 941 | 940 | 941 | 935 | 940 | 939 | 917 |
| Trait | ECV | | Stats: | Mean | 154.69 | SD | 18.1 | Min | 108.27 | Max | 248.01 | *N* | 941 | | |

[a]All trait values in mm, except for ECV, which is in cc.

## 3.2 | Research question 1

Examination of the pattern of covariate significance change for individual iEIDs from Models 1–3 sheds light on how variation in the cranium is affected by biological factors related to overall body mass, cranial size, and local cranial shape variation. For Model 1, only sex, age, and their interactions are considered potential covariates. Body mass is included in Model 2 and both body and cranial size are included in Model 3. As the morphological level at which analyses are conducted localizes, the proportion of $V_P$ explained by included covariates ($V_{cov}$) increases ($\bar{V}_{cov1} = 0.507 \pm 0.23$, $\bar{V}_{cov2} = 0.527 \pm 0.24$, $\bar{V}_{cov3} = 0.588 \pm 0.25$; Figure 3a and Supporting Information Table S2).

The pattern of $h^2_r$ does not change appreciably from one model to the next (Pearson $r_{1,2} = 0.96$, $r_{2,3} = 0.94$, $r_{1,3} = 0.91$; Figure 3b), demonstrating that the highly and lowly heritable traits are essentially the same regardless of whether allometric variation is retained or removed. However, because $V_{Pr}$ decreases from one model to the next ($V_{Pr} = V_P - V_{cov}$) while $h^2_r$ remains the same, by definition, removing allometric variation must result in a roughly proportionate decrease in $V_A$. This expectation is supported by comparing the geometric mean values for $V_A$ within each model: $\bar{V}_{A1} = 0.199 \pm 1.6$, $\bar{V}_{A2} = 0.173 \pm 1.7$, $\bar{V}_{A3} = 0.133 \pm 1.9$ (Figure 3c and Supporting Information Table S2). The reduction in $V_A$ is significant ($F = 5.36$, $p = 0.01$) and suggests that a portion of the genetic variation underlying the iEIDs also contributes to variation in body mass and cranial size.

The $\rho_G$ estimates also indicate that measures of size and craniofacial shape share genetic variation, as half of the iEIDs have an estimate of $\rho_G(\text{iEID, kg}) \geq 0.33$ (Table 4). In other words, depending on the trait, anywhere between 0.02% and 48% (mean = 15%) of additive genetic variation of body mass and craniofacial form is shared [shared $V_A = (\rho_G)^2$]. In general, the traits with the highest correlation coefficients tend to be in the posterior basicranium (LDBA and POBA) and the midface (PMPM and ZIMX) while those with the lowest are found in the anterior neurocranium (BRPT and PTPT) and ACB (CPSL). This suggests that genetic variation contributing to body mass variation may

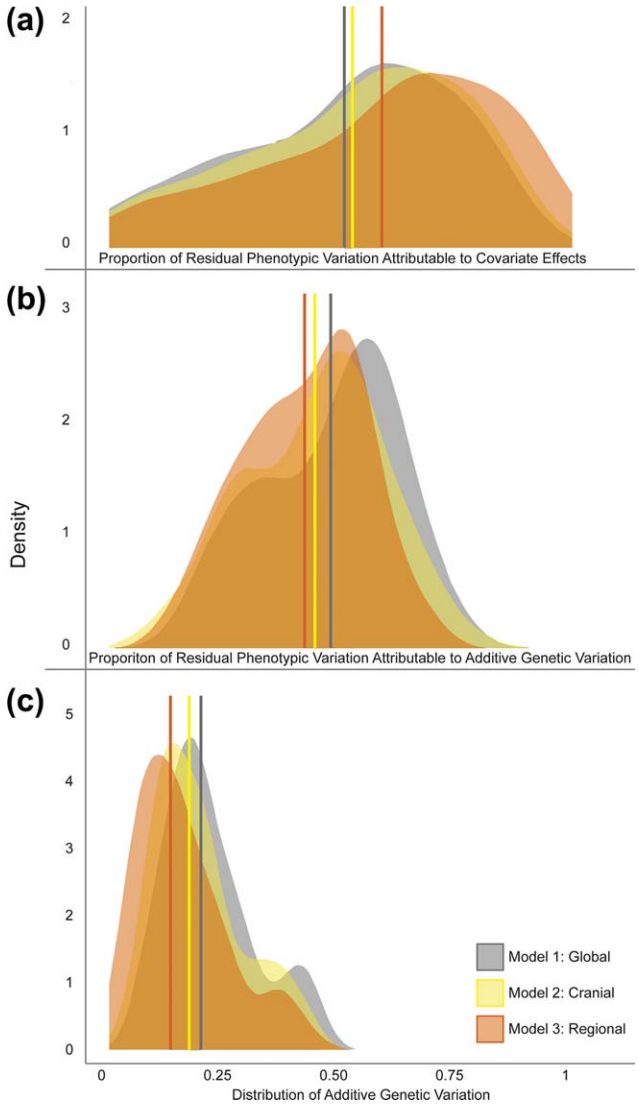


**FIGURE 3** Density plots for the estimated values of $V_{cov}$ (Panel A), $h_r^2$ (Panel B), and $V_A$ (Panel C) for the three nested covariate models. Average values are indicated by solid vertical lines of the same color as the corresponding density plot

not contribute uniformly to baboon craniofacial variation across the skull. Finally, Pearson correlations between $\rho_G$ and $h_r^2$ estimates from each model are low (Model 1: −0.10, Model 2: −0.27, Model 3: −0.24), indicating that strong correlation at the genetic level with body mass does not affect a trait's heritability estimate. This is significant as it indicates that examining relative heritability estimates alone is not sufficient to determine the basis of how traits respond to both direct and indirect selective pressures, for which knowledge of genetic correlations is of paramount importance (see also Houle, 1992).

The similarity matrix, $S_{ij}$, was constructed from the estimates of covariate effects. The degree to which the clusters reflect the true relationships among traits increased from Model 1 to 2 but did not differ between Models 2 and 3 (cophenetic correlation coefficient: $c_1 = 0.60$, $c_2 = 0.76$, $c_3 = 0.71$). Additionally, the pattern of the clusters changes among all three models (Supporting Information Fig. S1). Both results indicate that allometric variation structures baboon craniofacial variation such that removing it from downstream analyses alters the observed pattern of residual phenotypic variation. The most likely explanation for the different structures of the dendrograms created in each cluster analysis of model covariate effects is that allometric variation differentially affects cranial regions. This result is supported by the subsequent analysis of $\rho_G$ estimate distributions.

The distribution pattern of $\rho_G$ was compared among craniofacial regions to determine whether any contain a greater amount of genetic variation shared with body mass. The iEIDs were allocated to one of three general regions (face, base, and neurocranium) and to one of nine more specific regions corresponding more closely to functional modules, such as the orbits or the ACB (see Table 4). There was no pattern to the coefficients when dividing the cranium into three regions ($F = 0.16$, $p = 0.85$; Figure 4a). Overall, there was also no difference in the distribution pattern across the nine specific regions ($F = 1.17$, $p = 0.34$). However, closer examination of the coefficients within each specific region (Figure 4b) makes it obvious that the combination of significantly high $\rho_G$ estimates for global neurocranial traits (Welch's $t = 3.43$, df = 4.45, $p = 0.02$) and marginally low estimates for anterior neurocranial traits (Welch's $t = 2.20$, df = 3.76, $p = 0.10$) cancel each other out when grouped together into the general neurocranium category. This indicates that frontal bone form may be less affected by allometric variation, while measures of overall cranial size, such as neurocranial height or length, may be more affected.

### 3.3 | Research question 2

The effect of correlated responses in baboon craniofacial morphology resulting from direct selection on body mass alone was evaluated for a subset of 18 EIDs using their associated $\rho_G$(iEID, kg) estimates. The expected value for each craniofacial trait was calculated by transforming the average macaque cranium ($X_R$; Table 5) by the amount of correlated response to selection on body mass ($CR_y$). The resulting vector of simulated next generation mean phenotypes ($X_N$) was compared with the vector of observed mean baboon phenotypes ($X_B$; Table 5). If the selection intensity is very large ($i = 100$), the correlation between $X_N$ and $X_B$ is moderate in females ($r_F = 0.53$) and low in males ($r_M = 0.38$). If the intensity is set to 5.28 to account for the observed difference in mean adult body mass in macaques and baboons, the correlations increase slightly ($r_F = 0.61$, $r_M = 0.43$). In general, correspondence is low between the trait values observed in the SNPRC baboons and those calculated from the Cayo Santiago macaques after a single round of direct selection on body size (Figure 5).

## 4 | DISCUSSION

Quantitative genetic parameter estimates are specific to the sample selected, as the underlying genetic variation of traits is dependent on the presence and frequencies of alleles segregating within a population and the degree of environmental variation to which the population is subjected. Despite this, Hlusko and Mahaney (2007) have shown that, while the estimates may differ in value, the basic patterns of

**TABLE 4** Estimates of additive genetic correlations between adult body mass and each craniofacial trait, grouped by craniofacial region

| iEID[a] | Region[b] | $\rho_G \pm SE$ | iEID | Region | $\rho_G \pm SE$ | iEID | Region | $\rho_G \pm SE$ |
|---|---|---|---|---|---|---|---|---|
| BRNA | A | 0.343 ± 0.13 | SYBA | ACB | 0.198 ± 0.11 | ACSY | N | 0.306 ± 0.13 |
| *BRPT* | *A* | *0.097 ± 0.15* | VSBA | ACB | 0.256 ± 0.13 | FMPM | N | 0.453 ± 0.12 |
| *PTPT* | *A* | *0.094 ± 0.14* | ASJP | CFM | 0.545 ± 0.12 | NA41 | N | 0.545 ± 0.10 |
| STST | A | −0.297 ± 0.13 | BACC | CFM | 0.208 ± 0.14 | NAAC | N | 0.307 ± 0.12 |
| BRBA | G | 0.442 ± 0.12 | BAOP | CFM | 0.174 ± 0.13 | NANL | N | 0.336 ± 0.13 |
| **NALD** | **G** | **0.661 ± 0.12** | CNCN | CFM | 0.106 ± 0.16 | NAZI | N | 0.395 ± 0.12 |
| PTAS | G | 0.491 ± 0.14 | JPJP | CFM | 0.247 ± 0.11 | NLAC | N | 0.220 ± 0.14 |
| PTLD | G | 0.488 ± 0.14 | **LDBA** | **CFM** | **0.695 ± 0.08** | NLVS | N | 0.241 ± 0.12 |
| ASAS | P | 0.176 ± 0.17 | **POBA** | **CFM** | **0.613 ± 0.09** | ZSNL | N | 0.393 ± 0.12 |
| BRAS | P | 0.231 ± 0.15 | POPO | CFM | 0.437 ± 0.10 | CPZS | O | 0.531 ± 0.10 |
| BRLD | P | 0.398 ± 0.20 | 4141 | M | 0.381 ± 0.12 | DAFM | O | 0.163 ± 0.13 |
| LDAS | P | 0.196 ± 0.15 | 41MX | M | 0.397 ± 0.12 | FMCP | O | 0.514 ± 0.10 |
| CACP | ACB | 0.420 ± 0.16 | 41ZI | M | 0.536 ± 0.12 | FMPT | O | 0.268 ± 0.12 |
| *CPSL* | *ACB* | *0.019 ± 0.18* | ACPM | M | 0.578 ± 0.12 | NAFM | O | 0.233 ± 0.12 |
| NABA | ACB | 0.461 ± 0.11 | PLSY | M | 0.199 ± 0.13 | NAZS | O | 0.159 ± 0.13 |
| NACA | ACB | 0.314 ± 0.12 | *PM41* | *M* | *0.013 ± 0.17* | FMZT | Z | 0.353 ± 0.12 |
| NACP | ACB | 0.549 ± 0.10 | **PMPM** | **M** | **0.696 ± 0.15** | ZTPO | Z | 0.293 ± 0.25 |
| NAVS | ACB | 0.222 ± 0.13 | SYMX | M | 0.221 ± 0.14 | ZTVS | Z | 0.316 ± 0.13 |
| SLBA | ACB | 0.543 ± 0.14 | VSSY | M | 0.166 ± 0.13 | ZTZI | Z | 0.320 ± 0.17 |
| SLCC | ACB | 0.498 ± 0.13 | **ZIMX** | **M** | **0.668 ± 0.13** | ZTZT | Z | 0.397 ± 0.21 |

[a]iEIDs with particularly large estimates of $\rho_G$ (>|0.600|) are indicated in bold typeface and those with small estimates (<|0.100|) in italics.
[b]Traits are divided into three major cranial regions, each of which is further subdivided into specific regions. Neurocranium: anterior (A), global (G), posterior (P); basicranium: anterior cranial base (ACB), circum-foramen magnum (CFM); face: mouth (M), nose (N), orbits (O), malars/zygomas (Z).

phenotypic variation are markedly similar in captive and wild populations. This is to be expected because variation in both populations results from operation of the same underlying biological processes (see also Rodríguez-Clark, 2004). Here, we present a model of baboon evolution based on our analysis of a captive population that can be tested by incorporating data from wild and other captive populations.

## 4.1 | Covariate effects

Covariate effects were estimated to determine whether environmental factors explain any of the $V_P$ for individual traits and if so, to what degree. For all iEIDs and across all three levels of analysis, the proportion of $V_P$ explained by covariate effects ranged greatly, from 1.2% to 91.0%. The covariates that were most commonly significant among the traits considered include sex, body mass, and cranial size.

Although sex differences account for $V_P$ in a large proportion of iEIDs in every model, that amount decreased from 98% in Model 1 to 93% in Models 2 and 3. In addition, once body mass variation is removed the number of iEIDs with variance affected by other covariates decreases drastically. In Model 1, 47, 58, and 47% of iEIDs are affected by age-by-sex, age$^2$, and age$^2$-by-sex factors, respectively, but those numbers drop by approximately half in Models 2 and 3. This suggests that these covariates are representative of age and sex differences in body mass variation.

For example, about half of the iEIDs demonstrate significant age$^2$-by-sex effects in Model 1. It is well established that systemic hormone levels differ by sex and affect diverse biological processes (e.g., Gillies & McArthur, 2010; Goodman-Gruen & Barrett-Connor, 2000; Oertelt-Prigione, 2012; Pederson et al., 1999). For example, increased androgen levels differentially influence bone growth in early life and bone resorption later in life in a sex-specific manner (Clarke & Khosla, 2009). If $V_P$ varies with age because of differential gene expression and those genes affect hormones in males and females differently or those hormones have different effects on males and females, this could explain observed age$^2$-by-sex interaction effects. However, the number of iEIDs with such covariate effects is halved in Models 2 and 3, demonstrating that this age$^2$-by-sex interaction is mediated via the effect of allometry.

It is of note that the four posterior cranial vault traits (ASAS, BRAS, BRLD, and LDAS) show significant age$^2$ and age$^2$-by-sex effects in Model 1, but that these effects disappear once allometric variation is removed. These iEIDs delineate a craniofacial region that manifests

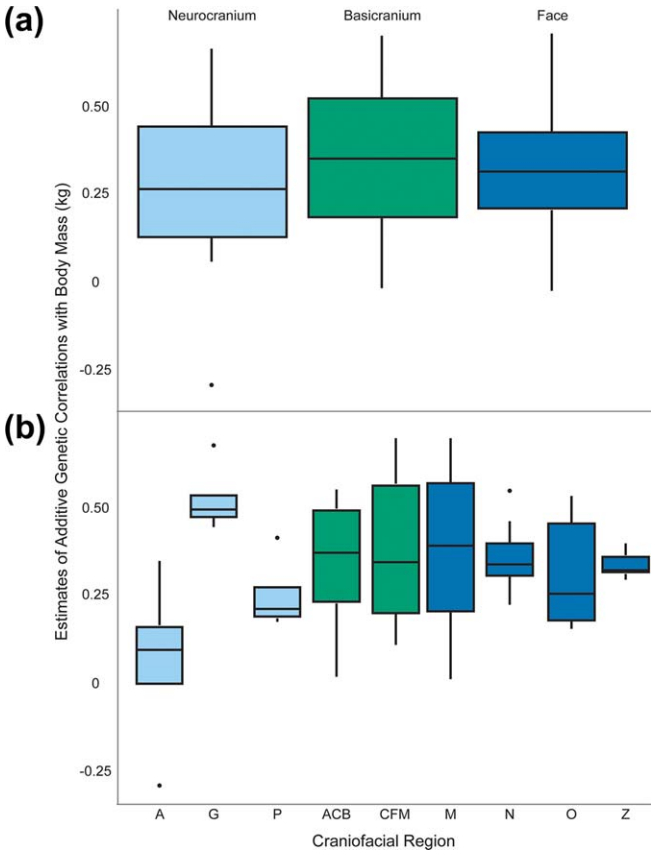


**FIGURE 4** Distribution of $\rho_G$ in different regions of the cranium. General categories are shown in Panel A and more specific ones in Panel B, which are colored according to the general craniofacial category in Panel A to which they correspond

prominent sagittal and nuchal crests in older adult males and is the only region in which all constituent iEIDs are affected by the same covariates in the same manner, explaining age$^2$ and age$^2$-by-sex as covariates. These effects completely disappear once body mass variation is controlled for in Models 2 and 3, suggesting the shape of these crests is solely allometric.

The only covariate that remains unaffected by the removal of allometric variation is age. Roughly, the same numbers of iEIDs show significant age-related effects in all three models (28, 30, and 32%, respectively). These results indicate that, although individuals have completed dental eruption and their basicranial growth centers have fused (i.e., the biological markers we selected to define "adulthood"), there is still a portion of the sample's $V_P$ that is explained by differences in craniofacial form among individuals of different ages, and this is particularly true in the ACB. Although it is typically assumed that craniofacial form is fixed in adults, except in cases of bone remodeling due to disease, trauma, and/or dental attrition, many studies have shown significant morphological change in the adult craniofacial complex (e.g., Formby, Nanda, & Currier, 1994; Hettena, 2004; Hrdlicka, 1936; Israel, 1968, 1973; Ruff, 1980; Vercauteren, 1990). A systematic study of age-related craniofacial variation in this sample, in which we have control over many variables, may be a worthwhile endeavor.

Finally, there are four traits whose variation is significantly affected by every potential covariate in all three models: 41ZI, ZIMX, FMPM, and ZTZT. These dimensions primarily describe midfacial breadth and, in particular, capture variation in the lateral flare of the malar region.

## 4.2 | Implications for allometric corrections

With few exceptions, the amount of $V_A$ reflected in a trait's $V_{Pr}$ decreased in Models 2 and 3 after accounting for global and local allometric effects, respectively. Given the number of genetic loci that have been identified affecting body mass (>250; Rankinen et al., 2006) and height (>400; Wood et al., 2014) variation in humans, and the fact that at least some, if not most, of these loci are pleiotropic and/or demonstrate epistasis (e.g., Brockman et al., 2000; Curran et al., 2013; Dong, Li, Li, & Price, 2005), it is not surprising that removing the proportion of phenotypic variation affected by body-size allometry removes the associated genetic information contributed by loci that also affect body-size variation.

This is a significant observation in the context of comparative analyses where some measure of overall size, such as body mass, cranial base length, or femoral length is often used to correct for both intra- and interspecific allometric effects. Our results indicate that the choice of measurement used for standardization and the scale at which trait variation is considered may affect the phylogenetic and selective signals of a trait. This should be no surprise, given that there is no unique

**TABLE 5** Mean trait values of 18 craniofacial dimensions for rhesus macaques and SNPRC baboons

| | Macaque | | Baboon | |
|---|---|---|---|---|
| Trait | Female | Male | Female | Male |
| BRNA | 51.63 | 53.80 | 61.57 | 64.68 |
| BRPT | 40.13 | 40.89 | 44.53 | 44.31 |
| PTPT | 48.12 | 49.14 | 58.25 | 58.90 |
| PTAS | 49.10 | 51.82 | 53.86 | 58.92 |
| PTLD | 61.77 | 63.84 | 68.33 | 73.62 |
| ASAS | 45.13 | 47.75 | 58.18 | 64.52 |
| BRAS | 50.43 | 52.08 | 58.78 | 64.41 |
| BRLD | 42.35 | 42.94 | 46.25 | 49.04 |
| LDAS | 28.28 | 29.23 | 36.36 | 44.37 |
| VSBA | 14.53 | 14.58 | 28.73 | 33.93 |
| ASJP | 24.76 | 27.27 | 38.19 | 41.60 |
| JPJP | 31.71 | 33.21 | 20.19 | 22.56 |
| LDBA | 43.00 | 44.52 | 57.76 | 68.02 |
| POPO | 22.41 | 23.73 | 72.81 | 88.73 |
| NANL | 17.32 | 19.03 | 53.57 | 71.79 |
| FMPT | 17.57 | 19.37 | 27.25 | 32.86 |
| FMZT | 30.97 | 34.36 | 33.71 | 39.32 |
| ZTZI | 20.46 | 23.29 | 19.24 | 25.80 |

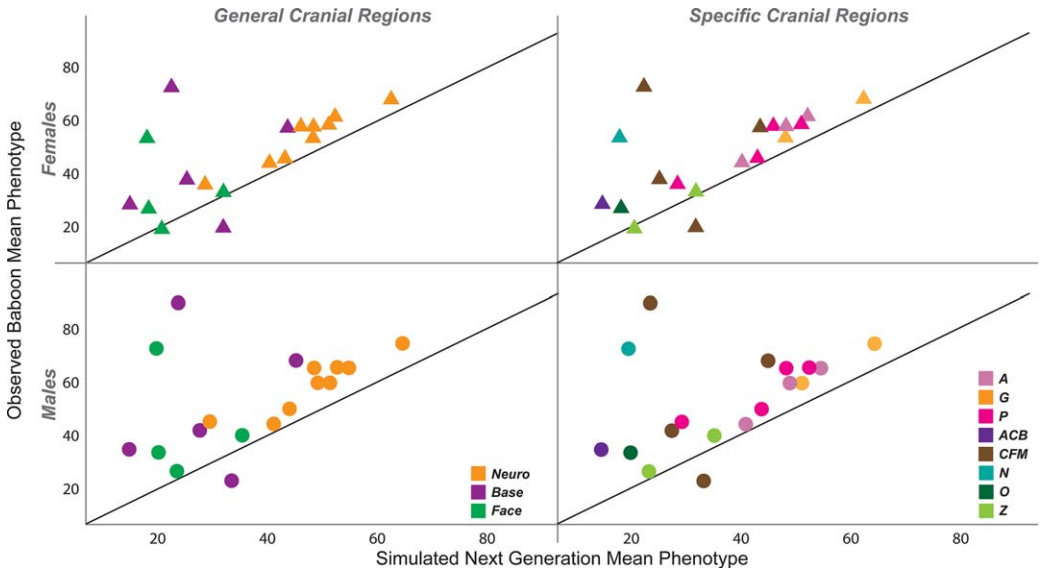


**FIGURE 5** Scatterplots of the sex-specific observed mean values for baboon craniofacial morphology against those values expected if indirect selection on body mass in ancestral papionins was the only force acting in baboon craniofacial evolution. The results shown are for the application of a selection intensity (*i*) equal to 5.28, or the number of standard deviations between mean adult body mass in male baboons and rhesus macaques, but those for $i = 100$ are very similar. The abbreviations in the color-coding legend for the specific cranial regions are the same as those given in Figure 2. The solid black line denotes x = y

or precise definition of size and that varied biological processes contribute to every chosen surrogate for the complex trait "size" (Richtsmeier et al., 2002). Consequently, several researchers have voiced concern about trait selection, arguing either for or against the use of measurements from certain cranial regions over others (e.g., Cardini & Elton, 2008; Harvati & Weaver, 2006; Olson, 1981; Roseman et al., 2010). Other investigators have discussed the relative merits of the myriad methods for allometric corrections (e.g., Jungers, 1985), particularly as they are applied (and often misapplied) statistically (e.g., Smith, 1981, 2005). Because every proxy trait for body size has a different set of underlying genes and these genes have varying pleiotropic effects spread throughout the cranium, the residual patterns of $V_A$ (observable as $V_P$) will depend on which proxy is selected for statistical allometric control. Therefore, any inferences about selective pressures or evolutionary processes that are drawn considering these differing $V_A$ patterns are potentially biased by the choice of body size proxy. To our knowledge, this is the first study to provide evidence of the effects of body mass on craniofacial variation via the presence of shared genetic variation, as was hypothesized by Hlusko, Weiss, and Mahaney (2002).

## 4.3 | Allometric variation and papionin evolution

One result of injudicious application of scaling methods is that estimated patterns of trait covariance could be drastically altered. This would lead to inaccurate interpretations as a result of conflating the effects of direct selection on one phenotype with indirect responses to selection on the traits with which it is correlated (Lande & Arnold, 1983). At least two large-scale changes in body size and facial projection characterize papionin evolution (one leading to the *Papio/Theropithecus* clade and the other to *Mandrillus*) and, given the short branches of the papionin phylogeny, these homoplasies evolved in parallel rather quickly (e.g., Gilbert & Rossie, 2007; Harris, 2000). One way to help explain these trends is by identifying genetic correlations underlying phenotypic variance patterns and ascertaining how such correlations bias evolutionary trajectories.

Our results suggest that genetic correlations between measures of craniofacial and body size variation are large enough to be biologically meaningful, such that selective pressures on one would have had salient concomitant effects on the other. These analyses cannot speak to directionality of the evolutionary trends and, therefore, selection may have been on either one or both sets of traits, or on traits we did not measure but that are genetically correlated with craniofacial and/or body size variation. Furthermore, craniofacial sexual dimorphism could have evolved either by increasing male body size and/or trait size or by decreasing or simply maintaining the size of such traits in females. If the genetic architecture of body size is similar in *Papio* and *Mandrillus*, which comparisons of genetic covariance matrices among other closely-related taxa suggest may be typical (e.g., Ackermann, 2002; Cheverud, 1989; de Oliveira, Porto, & Marroig, 2009; Marroig & Cheverud, 2001), then it is reasonable to hypothesize that similar selective pressures for increased body size operated on the two genera and contributed to their parallel craniofacial evolution.

Given that the craniofacial similarities among the large-bodied papionins appear to be dominated by midfacial traits, it is reasonable to hypothesize that such traits share more of their underlying genetic variation with body size than do others. Thus, selection on body size would have a proportionately greater indirect effect on baboon midfacial development, contributing to the observed homoplasy. However, we do not find evidence to support this as estimates of $\rho_G$ are not differentially distributed in baboon crania. In addition, we found a low

degree of correspondence between the observed and expected mean phenotypes when selecting on body mass alone (see Figure 5). These results suggest that, although genetic correlations between craniofacial traits and body mass have likely resulted in a degree of correlated evolution via indirect response to selection on body mass variation, more complicated scenarios involving additional targets or other scenarios of selection must be invoked to explain the craniofacial variation quantified in the SNPRC baboons. For example, it is entirely possible that unmeasured traits are negatively correlated with certain craniofacial traits, thus differentially counteracting the positive directional selection resulting from any correlations with body mass and producing a cranium that has experienced more change in only some regions from the ancestral condition.

In addition to highlighting the lack of correspondence between the mean baboon phenotypes and those after the macaque means underwent an episode of correlated response to body mass selection, our results also revealed that this lack of correspondence differs between the sexes. The lower correlations between observed and expected mean phenotypes for males indicate that they have likely undergone additional morphological evolution beyond that of their female counterparts. Whether that is the result of sex-specific selective pressures or a greater degree of genetic correlation between craniofacial and body mass variation in males is unknown but warrants further investigation.

Our analyses speak to the question of craniofacial evolution in papionins, but also have broader implications for understanding similar processes in nonprimate mammalian orders. If the genetic integration between craniofacial and body mass variation in this sample of baboons is indicative of a larger trend in the genetic architecture of mammalian crania, this may provide a mechanistic explanation for the recent suggestion that cranial evolutionary allometry (CREA) is a rule among mammals (Tamagnini, Meloro, & Cardini, 2017). CREA describes the tendency for larger taxa to have relatively longer faces than their smaller-bodied sister taxa. This has been demonstrated empirically to hold in felids, lagomorphs, papionins, some marsupials, and two clades of birds (Bright, Marugán-Lobón, Cobb, & Rayfield, 2016; Cardini, Polly, Dawson, & Milne, 2015; Fiorello & German, 1997; Linde-Medina, 2016; Singleton, 2002; Tamagnini et al., 2017). As the neurocranium and facial skeleton experience different growth trajectories postnatally, and body size growth is often non-linear, questions about both CREA in mammals and craniofacial homoplasy in papionins may be best addressed by focusing on the patterns of developmental timing that are shared between somatic and craniofacial growth trajectories.

## 5 | CONCLUSION

The aim of this research was to determine how phenotypic variation in the baboon cranium is differentially affected by genetic and environmental factors. Analyses were conducted at three different levels to examine how these effects change because of body and cranial size variation, sex, and age. Significant genetic correlations between body mass and craniofacial form provide evidence for the effects of pleiotropy in the genetic architecture of baboon craniofacial morphology and provide a possible mechanistic explanation for the co-occurrence of large body size and distinctive faces in the papionin clade.

## ACKNOWLEDGMENTS

The authors would like to thank Erik Trinkaus, Allan Larson, Rosemary Joganic, and three anonymous reviewers for comments provided on early drafts; Frank Brooks, Alexandre Gauvin, and Heather Lawson for help with SOLAR and Python script writing; Gary Schwartz and Teague O'Mara for providing their IPR script; and Richard Smith for stimulating discussions about allometric concerns. Body mass data were kindly provided by Anthony Comuzzie from the SNPRC. Funding for specimen curation and CT scan acquisition was provided by NSF BCS-0725068 and BCS-0523637 and for maintenance of the baboons by NIH P51RR013896, P01HL028972, and R01RR08781. All work was conducted in the Department of Anthropology at Washington University in St. Louis, Missouri.

Jessica L. Joganic curated and CT scanned a large portion of the skeletal sample, collected ECV and microscribe-based coordinate data, performed analyses, and wrote the manuscript. Katherine E. Willmore collected all digital landmark data. As PIs and Co-PIs on the NSF grants that supported this research, Joan T. Richtsmeier, Kenneth M. Weiss, Jeffrey Rogers, and James M. Cheverud were involved in the conception and initiation of the overall project, obtained and transported the sample individuals, directed data collection processes, and participated in ongoing analysis. Michael C. Mahaney, along with James M. Cheverud, aided in the running of statistical genetic analyses and interpretation of the results.

## ORCID

*Jessica L. Joganic* http://orcid.org/0000-0002-3245-4643
*Kenneth M. Weiss* http://orcid.org/0000-0002-2528-9993

## REFERENCES

Ackermann, R. R. (2002). Patterns of covariation in the hominoid craniofacial skeleton: implications for paleoanthropological models. *Journal of Human Evolution*, *43*, 167–187.

Ackermann, R. R., Rogers, J., & Cheverud, J. M. (2006). Identifying the morphological signatures of hybridization in primate and human evolution. *Journal of Human Evolution*, *51*, 632–645.

Ackermann, R. R., Schroeder, L., Rogers, J., & Cheverud, J. M. (2014). Further evidence for phenotypic signatures of hybridization in descendant baboon populations. *Journal of Human Evolution*, *76*, 54–62.

Almasy, L., & Blangero, J. (1998). Multipoint quantitative-trait linkage analysis in general pedigrees. *American Journal of Human Genetics*, *62*, 1198–1211.

Berner, D. (2011). Size correction in biology: how reliable are approaches based on (common) principal component analysis? *Oecologia*, *166*, 961–971.

Berry, D. P., Buckley, F., Dillon, P., Evans, R. D., Rath, M., & Veerkamp, R. F. (2003). Genetic parameters for body condition score, body

weight, milk yield, and fertility estimated from using random regression models. *Journal of Dairy Science*, *86*, 3704–3717.

Boissinot, S., Alvarez, L., Giraldo-Ramirez, J., & Tollis, M. (2014). Neutral nuclear variation in baboons (genus Papio) provides insight into their evolutionary and demographic histories. *American Journal of Physical Anthropology*, *155*, 621–634.

Bright, J. A., Marugán-Lobón, J., Cobb, S. N., & Rayfield, E. J. (2016). The shapes of bird beaks are highly controlled by nondietary factors. *Proceedings of the National Academy of Sciences of the United States of America*, *113*, 5352–5357.

Brockmann, G. A., Kratzsch, J., Haley, C. S., Renne, U., Schwerin, M., & Karle, S. (2000). Single QTL effects, epistasis, and pleiotropy account for two-thirds of the phenotypic F2 variance of growth and obesity in DU6i x DBA/2 mice. *Genome Research*, *10*, 1941–1957.

Burress, E. D. (2015). Cichlid fishes as models of ecological diversification: Patterns, mechanisms, and consequences. *Hydrobiologia*, *748*, 7–27.

Cardini, A., & Elton, S. (2008). Does the skull carry a phylogenetic signal? Evolution and modularity in the guenons. *Biological Journal of the Linnean Society*, *93*, 813–834.

Cardini, A., Polly, D., Dawson, R., & Milne, N. (2015). Why the long face? kangaroos and wallabies follow the same "rule" of cranial evolutionary allometry (CREA) as placentals. *Evolutionary Biology*, *42*, 169–176.

Carpentier, M. J. E., Fontaine, M. C., Cherel, E., Renoult, J. P., Jenkins, T., Benoit, L., ... Tung, J. (2012). Genetic structure in a dynamic baboon hybrid zone corroborates behavioral observations in a hybrid population. *Molecular Ecology*, *21*, 715–731.

Carson, E. A. (2006). Maximum likelihood estimation of human craniometric heritabilities. *American Journal of Physical Anthropology*, *131*, 169–180.

Cheverud, J. M. (1982). Phenotypic, genetic, and environmental morphological integration in the cranium. *Evolution*, *36*, 499–516.

Cheverud, J. M. (1989). A comparative analysis of morphological variation patterns in the papionins. *Evolution*, *43*, 1737–1747.

Cheverud, J. M. (1995). Morphological integration in the saddle-back tamarin (Saguinus fuscicollis) cranium. *American Naturalist*, *145*, 63–89.

Cheverud, J. M. (1996). Quantitative genetic analysis of cranial morphology in the cotton-top (Saguinus Oedipus) and saddle-back (S. fuscicollis) tamarins. *Journal of Evolutionary Biology*, *9*, 5–42.

Cheverud, J. M., & Buikstra, J. E. (1981a). Quantitative genetics of skeletal nonmetric traits in the rhesus macaques on Cayo Santiago. I. Single trait heritabilities. *American Journal of Physical Anthropology*, *54*, 43–49.

Cheverud, J. M., & Buikstra, J. E. (1981b). Quantitative genetics of skeletal nonmetric traits in the rhesus macaques on Cayo Santiago. II. Phenotypic, genetic, and environmental correlations between traits. *American Journal of Physical Anthropology*, *54*, 51–58.

Cheverud, J. M., & Buikstra, J. E. (1982). Quantitative genetics of skeletal nonmetric traits in the rhesus macaques on Cayo Santiago. III. Relative heritability of skeletal nonmetric and metric traits. *American Journal of Physical Anthropology*, *59*, 151–155.

Cheverud, J. M., Falk, D., Vannier, M., Konigsberg, L., Helmkamp, R. C., & Hildebolt, C. (1990). Heritability of brain size and surface features in rhesus macaques (Macaca mulatta). *Journal of Heredity*, *81*, 51–57.

Clarke, B. L., & Khosla, S. (2009). Androgens and bone. *Steroids*, *74*, 296–305.

Clutton-Brock, T. (2009). Sexual selection in females. *Animal Behaviour*, *77*, 3–11.

Clutton-Brock, T. H., & Harvey, P. H. (1977). Primate ecology and social organization. *Journal of Zoology*, *183*, 1–39.

Collard, M., & O'higgins, P. (2001). Ontogeny and homoplasy in the papionin monkey face. *Evolution & Development*, *3*, 322–331.

Collard, M., & Wood, B. (2000). How reliable are human phylogenetic hypotheses? *Proceedings of the National Academy of Sciences of the United States of America*, *97*, 5003–5006.

Cooper, W. J., & Westneat, M. W. (2009). Form and function of damselfish skulls: rapid and repeated evolution into a limited number of trophic niches. *BMC Evolutionary Biology*, *9*, 24.

Cotterman, C. W. (1940). A calculus for statistico-genetics (Doctoral dissertation). Columbus, OH: Ohio State University.

Curran, J. E., McKay, D. R., Winkler, A. M., Olvera, R. L., Carless, M. A., Dyer, T. D., ... Glahn, D. C. (2013). Identification of pleiotropic genetic effects on obesity and brain anatomy. *Human Heredity*, *75*, 136–143.

de Oliveira, F. B., Porto, A., & Marroig, G. (2009). Covariance structure in the skull of Catarrhini: A case of pattern stasis and magnitude evolution. *Journal of Human Evolution*, *56*, 417–430.

Disotell, T. R. (1992). Mitochondrial DNA phylogeny of the Old-World monkey tribe Papionini. *Molecular Biology and Evolution*, *9*, 1–13.

Dong, C., Li, W. D., Li, D., & Price, R. A. (2005). Interaction between obesity-susceptibility loci in chromosome regions 2p25-p24 and 13q13-q21. *European Journal of Human Genetics*, *13*, 102–108.

Dunbar, R. I. M. (1990). Environmental determinants of intraspecific variation in body weight in baboons (Papio spp.). *Journal of Zoology*, *220*, 157–169.

Falconer, D. S., & Mackay, T. F. C. (1996). *Introduction to quantitative genetics* (4th Ed.). Essex, GBR: Pearson Education Limited.

Fiorello, C. V., & German, R. Z. (1997). Heterochrony within species: Craniofacial growth in giant, standard, and dwarf rabbits. *Evolution*, *51*, 250–261.

Formby, W. A., Nanda, R. S., & Currier, G. F. (1994). Longitudinal changes in the adult facial profile. *American Journal of Orthodontics and Dentofacial Orthopedics*, *105*, 464–476.

Foster, J. B. (1964). Evolution of mammals on islands. *Nature*, *202*, 234–235.

Freedman, L. (1962). Growth of muzzle length relative to calvaria length in Papio. *Growth*, *26*, 117–128.

Freedman, L. (1963). A biometric study of Papio cynocephalus skulls from Northern Rhodesia and Nyasaland. *Journal of Mammalogy*, *44*, 24–43.

Frost, S. R., Marcus, L. F., Bookstein, F. L., Reddy, D. P., & Delson, E. (2003). Cranial allometry, phylogeography, and systematics of large-bodied papionins (Primates: Cercopithecinae) inferred from geometric morphometric analysis of landmark data. *The Anatomical Record. Part A, Discoveries in Molecular Cellular and Evolutionary Biology*, *275*, 1048–1072.

Gilbert, C. C. (2011). Phylogenetic analysis of the African papionin basicranium using 3-D geometric morphometrics: The need for improved methods to account for allometric effects. *American Journal of Physical Anthropology*, *144*, 60–71.

Gilbert, C. C., & Rossie, J. B. (2007). Congruence of molecules and morphology using a narrow allometric approach. *Proceedings of the National Academy of Sciences of the United States of America*, *104*, 11910–11914.

Gill, P. G., Purnell, M. A., Crumpton, N., Brown, K. R., Gostling, N. J., Stampanoni, M., & Rayfield, E. J. (2014). Dietary specializations and diversity in feeding ecology of the earliest stem mammals. *Nature*, *512*, 303–305.

Gillies, G. E., & McArthur, S. (2010). Estrogen actions in the brain and the basis for differential action in men and women: A case study for sex-specific medicines. *Pharmacological Reviews*, *62*, 155–198.

Goodman-Gruen, D., & Barrett-Connor, E. (2000). Sex differences in the association of endogenous sex hormone levels and glucose tolerance status in older men and women. *Diabetes Care*, *23*, 912–918.

Gould, S. J., & Lewontin, R. C. (1979). The spandrels of San Marco and the Panglossian paradigm: a critique of the adaptationist programme. *Proceedings of the Royal Society B Biological Sciences*, *205*, 581–598.

Gower, J. C. (1971). A general coefficient of similarity and some of its properties. *Biometrics*, *27*, 857–871.

Harris, E. E. (2000). Molecular systematics of the Old World monkey tribe Papionini: Analysis of the total available genetic sequences. *Journal of Human Evolution*, *38*, 235–256.

Harvati, K., & Weaver, T. D. (2006). Human cranial anatomy and the differential preservation of population history and climate signatures. *The Anatomical Record. Part A, Discoveries in Molecular, Cellular, and Evolutionary Biology*, *288*, 1225–1233.

Hettena, A. M. (2004). A three-dimensional analysis of age-related change in the adult craniofacial skeleton (Unpublished doctoral dissertation). Baltimore, MD: Johns Hopkins University.

Hlusko, L. J., & Mahaney, M. C. (2007). A multivariate comparison of dental variation in wild and captive populations of baboons (Papio hamadryas). *Archives of Oral Biology*, *52*, 195–200.

Hlusko, L. J., Weiss, K. M., & Mahaney, M. C. (2002). Statistical genetic comparison of two techniques for assessing molar crown size in pedigreed baboons. *American Journal of Physical Anthropology*, *117*, 182–189.

Honaker, J., King, G., & Blackwell, M. (2011). Amelia II: A program for missing data. *Journal of Statistical Software*, *7*, 1–47.

Houle, D. (1992). Comparing evolvability and variability of quantitative traits. *Genetics*, *130*, 195–204.

Hrdlicka, A. (1936). Growth during adult life. *Proceedings of the American Philosophical Society*, *76*, 847–897.

Israel, H. (1968). Continuing growth in the human cranial skeleton. *Archives of Oral Biology*, *13*, 133–137.

Israel, H. (1973). Age factor and the pattern of change in craniofacial structures. *American Journal of Physical Anthropology*, *39*, 111–128.

Joganic, J. L. (2016). A quantitative genetic analysis of craniofacial variation in baboons (Doctoral dissertation). St. Louis, Missouri: Washington University.

Jolly, C. J. (1970). The seed-eaters: A new model of hominind differentiation based on a baboon analogy. *Man*, *5*, 5–26.

Jolly, C. J. (2003). Commentary: Cranial anatomy and baboon diversity. *The Anatomical Record. Part A, Discoveries in Molecular, Cellular, and Evolutionary Biology*, *275*, 1043–1047.

Jolly, C. J., Burrell, A. S., Phillips-Conroy, J. E., Bergey, C., & Rogers, J. (2011). Kinda baboons (Papio kindae) and grayfoot chacma baboons (P. ursinus griseipes) hybridize in the Kafue river valley, Zambia. *American Journal of Primatology*, *73*, 291–303.

Jungers, W. L. ((1985). ). *Size and scaling in primate biology*. New York: Plenum Press.

Jungers, W. L., Falsetti, A. B., & Wall, C. E. (1995). Shape, relative size, and size-adjustments in morphometrics. *Yearbook of Physical Anthropology*, *38*, 137–161.

Klingenberg, C. P. (2016). Size, shape, and form: concepts of allometry in geometric morphometrics. *Development Genes and Evolution*, *226*, 113–137.

Kruuk, L. E. B., Slate, J., Pemberton, J. M., Brotherstone, S., Guinness, F., & Clutton-Brock, T. (2002). Antler size in red deer: Heritability and selection but no evolution. *Evolution*, *56*, 1683–1695.

Lande, R. (1979). Quantitative genetic analysis of multivariate evolution, applied to brain:body size allometry. *Evolution*, *33*, 402–416.

Lande, R., & Arnold, S. J. (1983). The measurement of selection on correlated characters. *Evolution*, *37*, 1210–1226.

Leigh, S. R. (2006). Cranial ontogeny of Papio baboons (Papio hamadryas). *American Journal of Physical Anthropology*, *130*, 71–84.

Leigh, S. R. (2007). Homoplasy and the evolution of ontogeny in papionin primates. *Journal of Human Evolution*, *52*, 536–558.

Leigh, S. R. (2009). Growth and development of baboons. In J. L. VandeBerg, S. Williams-Blangero, & S. D. Tardif (Eds.), *The baboon in biomedical research* (pp. 57–88). New York: Springer.

Leigh, S. R., & Cheverud, J. M. (1991). Sexual dimorphism in the baboon facial skeleton. *American Journal of Physical Anthropology*, *84*, 193–208.

Leutenegger, W., & Kelly, J. T. (1977). Relationship of sexual dimorphism in canine size and body size to social, behavioral, and ecological correlates in anthropoid primates. *Primates*, *18*, 117–136.

Linde-Medina, M. (2016). Testing the cranial evolutionary allometric "rule" in Galliformes. *Journal of Evolutionary Biology*, *29*, 1873–1878.

Lindenfors, P., & Tullberg, B. S. (1998). Phylogenetic analyses of primate size evolution: The consequences of sexual selection. *Biological Journal of the Linnean Society*, *64*, 413–447.

Lomolino, M. V. (1985). Body size of mammals on islands: The island rule reexamined. *The American Naturalist*, *125*, 310–316.

MacDonald, D. W. (2001). *The new encyclopedia of mammals*. Oxford, England: Oxford University Press.

Maples, W. R., & McKern, T. W. (1967). A preliminary report on classification of the Kenya baboon. In H. Vartborg (Ed.) *The baboon in medical research* (Vol. 2, pp. 13–22). Austin, TX: University of Texas Press.

Marroig, G., & Cheverud, J. M. (2001). A comparison of phenotypic variation and covariation patterns and the role of phylogeny, ecology, and ontogeny during cranial evolution of New World monkeys. *Evolution*, *55*, 2576–2600.

Martínez-Abadías, N., Esparza, M., Sjøvold, T., González-José, R., Santos, M., & Hernández, M. (2009). Heritability of human cranial dimensions: Comparing the evolvability of different cranial regions. *Journal of Anatomy*, *214*, 19–35.

Menegaz, R. A., Sublett, S. V., Figueroa, S. D., Hoffman, T. J., Ravosa, M. J., & Aldridge, K. (2010). Evidence for the influence of diet on cranial form and robusticity. *The Anatomical Record*, *293*, 630–641.

Mousseau, T. A., & Roff, D. A. (1987). Natural selection and the heritability of fitness components. *Heredity*, *59*, 181–197.

Oertelt-Prigione, S. (2012). The influence of sex and gender on the immune response. *Autoimmunity Reviews*, *11*, 479–485.

O'Higgins, P., & Collard, M. (2002). Sexual dimorphism and facial growth in papionin monkeys. *Journal of Zoology*, *257*, 255–272.

Olson, T. R. (1981). Basicranial morphology of the extant hominoids and Pliocene hominids: the new material from the Hadar Formation, Ethiopia and its significance in early human evolution and taxonomy. In C. B. Stringer (Ed.), *Aspects of human evolution* (pp. 99–128). London, GBR: Taylor and Francis.

O'Mara, M. T., Gordon, A. D., Catlett, K. K., Terranova, C. J., & Schwartz, G. T. (2012). Growth and the development of sexual size dimorphism in lorises and galagos. *American Journal of Physical Anthropology*, *147*, 11–20.

Pederson, L., Kremer, M., Judd, J., Pascoe, D., Spelsberg, T. C., Riggs, B. L., & Oursler, M. J. (1999). Androgens regulate bone resorption activity of isolated osteoclasts in vitro. *Proceedings of the National Academy of Sciences of the United States of America*, *96*, 505–510.

Plavcan, J. M., & van Schaik, C. P. (1992). Intrasexual competition and canine dimorphism in anthropoid primates. *American Journal of Physical Anthropology*, *87*, 461–477.

Plavcan, J. M., & van Schaik, C. P. (1997). Intrasexual competition and body weight dimorphism in anthropoid primates. *American Journal of Physical Anthropology*, *103*, 37–68.

Plavcan, J. M., van Schaik, C. P., & Kappeler, P. M. (1995). Competition, coalitions and canine size in priamtes. *Journal of Human Evolution*, *28*, 245–276.

Porto, A., de Oliveira, F. B., Shirai, L. T., De Conto, V., & Marroig, G. (2009). The evolution of modularity in the mammalian skull I: Morphological integration patterns and magnitudes. *Evolutionary Biology*, *36*, 118–135.

Rankinen, T., Zuberi, A., Chagnon, Y. C., Weisnagel, S. J., Argyropoulos, G., Walts, B., … Bouchard, C. (2006). The human obesity gene map: The 2005 update. *Obesity*, *14*, 529–644.

Richtsmeier, J. T., DeLeon, V. B., & Lele, S. R. (2002). The promise of geometric morphometrics. *Yearbook of Physical Anthropology*, *119*, 63–91.

Rodríguez-Clark, K. M. (2004). Effect of captivity on genetic variance for five traits in the large milkweed bug (Oncopeltus fasciatus). *Heredity*, *93*, 51–61.

Roseman, C. C., Willmore, K. E., Rogers, J., Hildebolt, C., Sadler, B. E., Richtsmeier, J. T., & Cheverud, J. M. (2010). Genetic and environmental contributions to variation in baboon cranial morphology. *American Journal of Physical Anthropology*, *143*, 1–12.

Rosvall, K. A. (2011). Intrasexual competition in females: Evidence for sexual selection? *Behavioral Ecology*, *22*, 1131–1140.

RStudio Team. (2016). RStudio: Integrated development for R. Boston, MA: RStudio Inc. http://www.rstudio.com/

Ruff, C. B. (1980). Age differences in craniofacial dimensions among adult from Indian Knoll, Kentucky. *American Journal of Physical Anthropology*, *53*, 101–108.

Safari, E., Fogarty, N. M., & Gilmour, A. R. (2005). A review of genetic parameter estimates for wool, growth, meat and reproduction traits in sheep. *Livestock Production Science*, *92*, 271–289.

Sherwood, R. J., Duren, D. L., Demerath, E. W., Czerwinski, S. A., Siervogel, R. M., & Towne, B. (2008). Quantitative genetics of modern human cranial variation. *Journal of Human Evolution*, *54*, 909–914.

Singleton, M. (2002). Patterns of cranial shape variation in the Papionini (Primates: Cercopithecinae). *Journal of Human Evolution*, *42*, 547–578.

Singleton, M. (2012). Postnatal cranial development in papionin primates: An alternative model for hominin evolutionary development. *Journal of Evolutionary Biology*, *39*, 499–520.

Smith, R. J. (1981). On the definition of variables in studies of primate dental allometry. *American Journal of Physical Anthropology*, *55*, 323–329.

Smith, R. J. (2005). Relative size versus controlling for size: Interpretation of ratios in research on sexual dimorphism in the human corpus callosum. *Current Anthropology*, *46*, 249–273.

Smith, F. A., Boyer, A. G., Brown, J. H., Costa, D. P., Dayan, T., Morgan Ernest, S. K., … Uhen, M. D. (2010). The evolution of maximum body size of terrestrial mammals. *Science*, *330*, 1216–1219.

Smith, H. F., & von Cramon-Taubadel, N. (2015). The relative correspondence of cranial and genetic distances in papionin taxa and the impact of allometric adjustments. *Journal of Human Evolution*, *85*, 46–64.

Steppan, S. J., Phillips, P. C., & Houle, D. (2002). Comparative quantitative evolution of the G matrix. *Trends in Ecology & Evolution*, *17*, 320–327.

Tamagnini, D., Meloro, C., & Cardini, A. (2017). Anyone with a long-face? Craniofacial evolutionary allometry (CREA) in a family of short-face mammals, the Felidae. *Evolutionary Biology*, *44*, 476–495.

Tosi, A. J., Disotell, T. R., Morales, J. C., & Melnick, D. J. (2001). Cercopithecine Y-chromosome data provide a test of competing morphological evolutionary hypotheses. *Molecular Phylogenetics and Evolution*, *27*, 510–521.

Van Valen, L. (1973). Pattern and the balance of nature. *Evolutionary Theory*, *1*, 31–49.

Vercauteren, M. (1990). Age effects and secular trend in a cross-sectional sample: Application to four head dimensions in Belgian adults. *Human Biology*, *62*, 681–688.

Visscher, P. M., Thompson, R., & Hill, W. G. (1991). Estimation of genetic and environmental variances for fat yield in individual herds and an investigation into heterogeneity of variance between herds. *Livestock Production Science*, *28*, 273–290.

Wilder, H. H. (1920). *A laboratory manual of anthropometry*. Philadelphia, PA: P. Blakiston's Son & Company.

Willmore, K. E., Roseman, C. C., Rogers, J., Richtsmeier, J. T., & Cheverud, J. M. (2009). Genetic variation in baboon craniofacial sexual dimorphism. *Evolution*, *63*, 799–806.

Wood, A. R., Esko, T., Yang, J., Vedantam, S., Pers, T. H., Gustafsson, S., … Frayling, T. M. (2014). Defining the role of common variation in the genomic and biological architecture of adult human height. *Nature Genetics*, *46*, 1173–1186.

Zinner, D., Groeneveld, L. F., Keller, C., & Roos, C. (2009). Mitochondrial phylogeography of baboons (Papio spp.): Indication for introgressive hybridization? *BMC Evolutionary Biology*, *9*, 83.

Zinner, D., Wertheimer, J., Liedigk, R., Groeneveld, L. F., & Roos, C. (2013). Baboon phylogeny as inferred from complete mitochondrial genomes. *American Journal of Physical Anthropology*, *150*, 133–140.

## SUPPORTING INFORMATION

Additional Supporting Information may be found online in the supporting information tab for this article.

**How to cite this article:** Joganic JL, Willmore KE, Richtsmeier JT, et al. Additive genetic variation in the craniofacial skeleton of baboons (genus *Papio*) and its relationship to body and cranial size. *Am J Phys Anthropol*. 2018;165:269–285. https://doi.org/10.1002/ajpa.23349